

**Bryn Mawr College**  
**Scholarship, Research, and Creative Work at Bryn Mawr**  
**College**

---

Physics Faculty Research and Scholarship

Physics

---

2012

# Methyl Group Rotation, H-1 Spin-Lattice Relaxation in an Organic Solid, and the Analysis of Nonexponential Relaxation

Peter A. Beckmann

*Bryn Mawr College*, [pbeckman@brynmawr.edu](mailto:pbeckman@brynmawr.edu)

Evan Schneider

[Let us know how access to this document benefits you.](#)

Follow this and additional works at: [http://repository.brynmawr.edu/physics\\_pubs](http://repository.brynmawr.edu/physics_pubs)

 Part of the [Physics Commons](#)

---

## Custom Citation

P. A. Beckmann and E. Schneider, *J. Chem. Phys.* **136**, 054508 (2012).

This paper is posted at Scholarship, Research, and Creative Work at Bryn Mawr College. [http://repository.brynmawr.edu/physics\\_pubs/49](http://repository.brynmawr.edu/physics_pubs/49)

For more information, please contact [repository@brynmawr.edu](mailto:repository@brynmawr.edu).

# Methyl group rotation, $^1\text{H}$ spin-lattice relaxation in an organic solid, and the analysis of nonexponential relaxation

Peter A. Beckmann<sup>a)</sup> and Evan Schneider<sup>b)</sup>

Department of Physics, Bryn Mawr College, 101 North Merion Avenue, Bryn Mawr, Pennsylvania 19010-2899, USA

(Received 26 July 2011; accepted 20 December 2011; published online 6 February 2012)

We report  $^1\text{H}$  spin-lattice relaxation measurements in polycrystalline 4,4'-dimethoxybiphenyl at temperatures between 80 and 300 K at NMR frequencies of  $\omega_0/2\pi = 8.50, 22.5,$  and  $53.0$  MHz. The data are interpreted in terms of the simplest possible Bloch-Wangsness-Redfield methyl group hopping model. Different solid states are observed at low temperatures. The  $^1\text{H}$  spin-lattice relaxation is nonexponential at higher temperatures where a stretched-exponential function fits the data very well, but this approach is phenomenological and not amenable to theoretical interpretation. (We provide a brief literature review of the stretched-exponential function.) The Bloch-Wangsness-Redfield model applies *only* to the relaxation rate that characterizes the initial  $^1\text{H}$  magnetization decay in a high-temperature nonexponential  $^1\text{H}$  spin-lattice relaxation measurement. A detailed procedure for determining this initial relaxation rate is described since large systematic errors can result if this is not done carefully. © 2012 American Institute of Physics. [doi:10.1063/1.3677183]

## I. INTRODUCTION

Experiments involving methyl group ( $\text{CH}_3$ ) dynamics and the models derived from these experiments provide information on intramolecular and intermolecular interactions in van der Waals molecular solids. At temperatures below approximately 80 K in most solids, the models for methyl group dynamics involve quantum mechanical tunneling<sup>1–9</sup> and the idea of the classical rotation of a triangle of spin-1/2 protons makes no sense. Indeed, the concepts of instantaneous position and speed have no place in the fundamental quantum mechanics of bound systems. Parameters such as correlation times and activation energies emerge through detailed calculations of quantum mechanical expectation values and the use of the canonical ensemble. Above approximately 80 K in most solids, however, the classical hopping of a triangle of protons<sup>3–5,7,10–14</sup> is an excellent model for the interpretation of nuclear magnetic resonance (NMR) relaxation data and has withstood the test of time.<sup>15–20</sup> In this model, we do indeed picture the triangle of spins as hopping from one equilibrium position to another in a  $3m$ -fold barrier for  $m = 1, 2, \dots$ . Whereas the low-temperature tunneling model is a very clear quantum mechanical model, the high-temperature classical hopping model is a typical quantum-classical hybrid. It is quantum mechanical in the sense that the three-proton wave function can be thought of as being highly localized (thus defining “positions”). In addition, the three protons jump instantaneously from one equilibrium position to another, meaning that there is no “motion” in the classical sense. This model is classical in that one can calculate

potential energy functions and think of the methyl group as continuously exchanging kinetic and potential energy as it rotates. One speaks of equilibrium structures (atomic positions) and transition structures. These two approaches seem internally inconsistent; the terms “instantaneous jump” and “continuous rotation” both appear (or are implied) at various places in the model. We just need to admit that the problem is with language, not with the mathematical models. Indeed, kinetic and potential energy have no place in the quantum mechanics of bound systems. There is only energy. So, the high-temperature region for methyl group dynamics seems confusing, but the mathematical model and the very small number of parameters that emerge, as reviewed below, are clear and well defined. We note that the transition from the low-temperature quantum mechanical tunneling regime to the high-temperature classical hopping regime is well understood.<sup>2–4,10,11,13</sup> We do note an interesting  $^1\text{H}$  spectroscopy study in a single crystal of partially deuterated methylmalonic acid [ $\text{CDCH}_3(\text{COOD})_2$ ] where, for spectra in the range 69–104 K, using a quantum-mechanical model for methyl group rotation gave a better fit of the data than the classical hopping model.<sup>21</sup> In the end, the tests of the validity of a model are (1) whether or not it is consistent with a wide variety of experimental results and (2) that it has a reasonably small number of adjustable parameters, all of which can be determined uniquely by the experiment.

Here, we report solid state NMR  $^1\text{H}$  spin-lattice relaxation experiments in polycrystalline 4,4'-dimethoxybiphenyl. (The molecule is shown as an inset in Fig. 1.) The experiments are performed at temperatures above 80 K and we use the classical (i.e., the quantum-classical hybrid) methyl group hopping model to interpret the data. The data covers a large temperature range at three NMR frequencies and only three adjustable parameters appear in the model. All three parameters are highly constrained by independent models. This

<sup>a)</sup> Author to whom correspondence should be addressed. Electronic mail: pbeckman@brynmawr.edu.

<sup>b)</sup> Present address: Department of Astronomy, University of Arizona, 933 North Cherry Avenue, Room N204, Tucson, Arizona 85721-0065, USA.

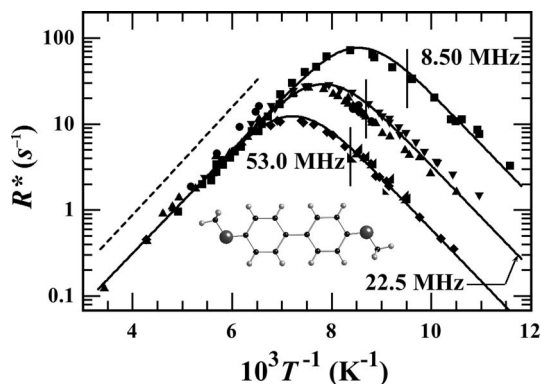


FIG. 1. The stretched-exponential characteristic  $^1\text{H}$  relaxation rate,  $R^*$ , versus inverse temperature,  $T^{-1}$ , in polycrystalline 4,4'-dimethoxybiphenyl at NMR frequencies  $\omega_0/2\pi = 8.50$  (■), 22.5 (▲, ▼, ●), and 53.0 MHz (◆, ◆, ◆). The inset shows the molecule. The different symbols for 22.5 and 53.0 MHz indicate different groupings of experiment days indicating (at lower temperatures) slightly different structures on different groups of days. At temperatures below (i.e., to the right of) the approximate positions of the vertical lines, the stretching parameter  $\beta > 0.95$  (see Fig. 4). At these temperatures, the stretched-exponential relaxation fit and a single-exponential relaxation fit, characterized by  $R$ , are indistinguishable ( $R^* = R$ ). The experimental uncertainties are within the sizes of the symbols. The solid lines correspond to a single fit as discussed in the text. The dashed line indicates the high-temperature  $R_S$  values in Fig. 2. The data to the right of the vertical lines are the same in Figs. 1 and 2 and are shown on an expanded scale in Fig. 3.

project represents a very strong test of the “classical” methyl group hopping model.

Above 100–120 K (depending on the NMR frequency), the  $^1\text{H}$  spin-lattice relaxation in this study is nonexponential for well-understood reasons.<sup>22,23</sup> A main thrust of this paper is to present a detailed look at the analysis of these  $^1\text{H}$  solid state NMR nonexponential relaxation data. If care is not taken, significant systematic errors in reported values of relaxation rates can result. Though the molecule itself is of little significance to the best of our knowledge, the analysis of nonexponential relaxation is an important general problem in many fields of science. Characterizing this relaxation using a stretched-exponential function<sup>24</sup> is very precise, but the relaxation rate that corresponds to meaningful theoretical models is the less precisely determined rate that characterizes the initial recovery curve of a perturbed nuclear magnetization.<sup>22,23</sup> (As a byproduct of this project, we provide a brief literature review of the stretched-exponential function in Sec. IV B.) Between 80 K and 100–120 K, again depending on the NMR frequency, the  $^1\text{H}$  spin-lattice relaxation is exponential. In this paper, we discuss the procedure for extracting meaningful dynamical parameters from the entire temperature and NMR frequency dependence of the relaxation. Elsewhere, we relate the observed barrier for methyl group rotation determined here to both the molecular and crystal structure of 4,4'-dimethoxybiphenyl.<sup>25</sup>  $^1\text{H}$  spin relaxation involves the modulation of both intramolecular and intermolecular  $^1\text{H}$  spin– $^1\text{H}$  spin interactions and as such is sensitive to small changes in the solid state, either crystal structure or molecule conformation (or both). Thus, we are able to observe polycrystalline 4,4'-dimethoxybiphenyl in different states on different days as a consequence of different thermal histories.<sup>26–30</sup>

## II. EXPERIMENTAL METHODS

The sample of 4,4'-dimethoxybiphenyl was purchased from Sigma Aldrich and further purified by recrystallization from 95% ethanol. Solid state  $^1\text{H}$  spin-lattice relaxation measurements were made between 80 and 300 K at NMR frequencies of  $\omega_0/2\pi = 8.50$ , 22.5, and 53.0 MHz (corresponding to magnetic fields of 0.200, 0.528, and 1.24 T).  $^1\text{H}$  magnetization recovery curves were measured using an inversion-recovery pulse sequence. Low NMR frequencies are used in these NMR relaxation studies to bring the methyl group mean hop rates into resonance with the NMR frequencies at reasonable temperatures. This is to be contrasted with the high NMR frequencies used in NMR spectroscopy measurements in order to better resolve chemical shifts and other interactions.

Temperature was controlled by a flow of cold nitrogen gas that could be heated to obtain the desired temperature. Temperature was measured with homemade silver-soldered copper-constantan thermocouples that were imbedded in the samples 2 mm outside the end of the 15 mm long, 7 mm diameter NMR coil. The many thermocouples used in the laboratory are carefully calibrated every few years using standard temperature references. They have not varied over a 25-year period. There is typically a 0.5 K gradient along the 15 mm of sample in the coil. Absolute temperatures are measured to  $\pm 2$  K and temperature differences are monitored to  $\pm 0.2$  K. Four thermocouples were used with two different samples at three different NMR frequencies (each with its own probe) at two complete (and independent) experimental stations. Three of the four thermocouples were used with both samples at all three frequencies. Observations were made at  $\omega_0/2\pi = 22.5$  and 53.0 MHz at one station and at 8.50 and 22.5 MHz at the other.

The free induction decay following a  $\pi/2$  observation pulse is not strictly exponential<sup>31</sup> in a polycrystalline sample but can be characterized by the time to decay to approximately  $1/e$  of the maximum height observed after the amplifier recovery. This time was approximately  $7 \mu\text{s}$  and varied very little over the entire temperature range studied. This corresponds to an NMR line width of approximately 450 kHz.

## III. NMR RELAXATION REVIEW AND THE NMR PARAMETERS

### A. Spin-1/2 spin-lattice relaxation

Abragam<sup>31</sup> describes the nuclear spin relaxation for an ensemble of isolated interacting pairs of spin-1/2 nuclei whose internuclear vectors are of fixed lengths but are re-orienting randomly. The spin-lattice relaxation rate for this system is strictly exponential. Abragam also reviews developments prior to about 1960, including the important contributions from Bloembergen, Purcell, and Pound,<sup>32</sup> Solomon,<sup>33</sup> Redfield,<sup>34</sup> Tomita,<sup>35</sup> Bloch,<sup>36</sup> and Wangsness and Bloch.<sup>37</sup> Additional important contributions in this early epoch were made by Woessner<sup>38</sup> and by Stejskal and Gutowsky.<sup>14</sup> Later developments along with appropriate references appear in the texts by Slichter,<sup>39</sup> Ernst *et al.*,<sup>40</sup> and Kimmich.<sup>41</sup> Goldman<sup>42</sup> has produced a recent review of the formalism. We refer to the current approach as the Bloch-Wangsness-Redfield theory of

nuclear spin relaxation,<sup>34,36,37</sup> which is beautifully summarized in a detailed manner by Kimmich.<sup>41</sup>

## B. The origin of the nonexponential relaxation at high temperatures

The nuclear spin-lattice relaxation resulting from the reorientation of a methyl group is complicated by the fact that the reorientation of the three spin-spin vectors in a methyl group is neither random nor uncorrelated. First, there are three spins and eight spin states. Second, in a solid, each triangle of spins reorients in a plane, not isotropically. Third, the motion of the three spin-spin vectors is 100% correlated. Runnells<sup>22</sup> and Hilt and Hubbard<sup>23</sup> dealt with these complications in detail and the result for an ensemble of isolated methyl groups oriented in the same direction (with respect to the applied magnetic field) is that the relaxation proceeds as the sum of four exponentials. This perturbed magnetization decay can be expressed in algebraic form as a function of the angle between the single methyl group rotation axis and the applied magnetic field. Although no experiment could ever observe four exponentials (which would involve at least nine adjustable parameters), nonexponential <sup>19</sup>F relaxation has been observed in a single crystal of CF<sub>3</sub>COOAg.<sup>43</sup> Hilt and Hubbard<sup>23</sup> performed a numerical averaging over all orientations of the methyl group reorientation axes appropriate for a polycrystalline powder and found that the relaxation is still nonexponential, particularly near the relaxation rate maximum and at higher temperatures. This has been observed in the work reported here and previously in other polycrystalline solids.<sup>44,45</sup>

Early experiments where nonexponentiality was observed were performed on solid samples made of small molecules (compared with 4,4'-dimethoxybiphenyl). In these samples, motions, such as whole-molecule tumbling in the solid state, are occurring on the NMR time scale (approximately 10<sup>-12</sup> to 10<sup>-5</sup> s in our case) in addition to methyl group motion.<sup>44-46</sup> The degree to which the relaxation is nonexponential depends on the relative time scales of the two motions (methyl group rotation and molecular tumbling) as well as on the geometry of the molecule.<sup>47</sup> The presence of either <sup>1</sup>H spin-spin interactions between methyl group protons and other protons or between protons on different methyl groups makes the relaxation more exponential.<sup>45,48</sup> This has been born out in experiments with solids comprised of larger organic molecules with several or many static (on the NMR time scale) hydrogen atoms. In many of these cases, the departure from exponential relaxation is very slight or not observed at all.<sup>49-53</sup> Polycrystalline 4,4'-dimethoxybiphenyl, however, seems to be an exception.

Finally, it has been shown that when the relaxation is nonexponential, the rate constant that characterizes the initial recovery of the nuclear magnetization following a perturbation is the rate predicted by the Bloch-Wangsness-Redfield model.<sup>22,44</sup> So, at short times following a perturbation, the effect of the correlations among the three spin-spin vectors does not come into play.

We note that the nonexponentiality at higher temperatures does *not* result from the lack of spin diffusion. The NMR spectrum is a very wide line (hundreds of kHz) over the en-

tire temperature range studied. This is to be compared with chemical shift differences of approximately 100s of Hz or less for all the protons involved in these organic molecular solids. A common spin temperature is maintained on the time scale of the inverse line width, even at the highest temperatures studied.

## C. Theoretical expressions for the relaxation rate and the origin of the fitting parameters

The relaxation rate (appropriate for 4,4'-dimethoxybiphenyl) is given by<sup>20,31</sup>  $R = (n/N) C [J(\omega_0, \tau) + 4J(2\omega_0, \tau)]$ . This expression is appropriate at temperatures between 80 and 100–120 K (depending on the NMR frequency) where the relaxation is exponential. At higher temperatures, this expression is appropriate for the rate that characterizes the initial recovery of the nonexponential relaxation. The constant  $C$  corresponds conceptually to the overall strength of the <sup>1</sup>H–<sup>1</sup>H spin-spin interactions that are being modulated by methyl group rotation (and any other motion that may be occurring on the NMR time scale). Considering only intramethyl <sup>1</sup>H–<sup>1</sup>H spin-spin interactions,  $C$  takes on the value  $\tilde{C} = (9/40)(\mu_0/4\pi)^2(\hbar\gamma^2/r^3)^2$  for <sup>1</sup>H magnetogyric ratio,  $\gamma$ , and intramethyl H–H distance,  $r$ .  $\mu_0$  is the magnetic constant. The various numerical factors that go into the ratio 9/40 are discussed elsewhere.<sup>16</sup>  $C/\tilde{C}$  is then treated as a fitting parameter and should be of order unity since the intramethyl H–H distances are usually significantly shorter than methyl H–nonmethyl H distances and  $R$  is proportional to  $r^{-6}$ . Using the factor,  $n/N$ , in the above expression is an approximation and assumes that spin diffusion, characterized by a rate  $(7 \mu\text{s})^{-1} = 1.4 \times 10^5 \text{ s}^{-1}$  over the entire temperature range studied (as discussed above) is much larger than the maximum value of the spin-lattice relaxation which is  $R \approx 10^2 \text{ s}^{-1}$ . That is, the energy-preserving spin-spin interactions (with small contributions from phonons) between the mobile  $n$  <sup>1</sup>H nuclei and the immobile  $(N - n)$  <sup>1</sup>H nuclei maintains the spin system at a common spin temperature. Another way to think of this is that all  $N$  <sup>1</sup>H nuclei are equally affected by the perturbation in the inversion-recovery experiment but the  $N - n$  immobile <sup>1</sup>H nuclei are only relaxed via the  $n$  mobile protons. This is an approximation because there are time dependent spin-spin interactions between methyl <sup>1</sup>H nuclei and nearby immobile <sup>1</sup>H nuclei. But, again, their distances are generally large compared with the intramethyl <sup>1</sup>H nuclear–<sup>1</sup>H nuclear distance and their dynamics involve small angular oscillations.

$J(\omega, \tau)$  is the spectral density,<sup>54</sup> which can be interpreted conceptually as the distribution of methyl group rotation (angular) frequencies,  $\omega$ , with  $\tau^{-1}$  being the mean (angular) frequency. This frequency  $\omega/2\pi$  is not to be confused with the NMR frequency  $\omega_0/2\pi$ . The motion of the magnetic dipoles (spins) produces a time-dependent magnetic field and the same spin system relaxes via the  $\omega = \omega_0$  Fourier component (single spin flips) and the  $\omega = 2\omega_0$  Fourier component (double spin flips) of this field. (See Hoult<sup>55</sup> for a very detailed discussion concerning what is happening, what is *not* happening, what should be said, and what should *not* be said, concerning the observation of an NMR signal. Also, see Engelke<sup>56</sup> for a

discussion of the role of virtual photons in a quantum field theoretic description of the detection of an NMR signal.)

The correlation time (the mean time between instantaneous methyl group rotational hops) is assumed to be given by an Arrhenius relation  $\tau = \tau_\infty \exp(E_{\text{NMR}}/kT)$  for NMR activation energy,  $E_{\text{NMR}}$ , and “infinite temperature correlation time”,  $\tau_\infty$ . This Arrhenius relation is also an approximation as discussed extensively by Clough and Heidemann<sup>13</sup> but is a good approximation so long as the NMR activation energy  $E_{\text{NMR}} \gg kT$ . (For the relaxation study presented here,  $E_{\text{NMR}}/kT$  varies from approximately 16 at the lowest temperatures to approximately 5 at the highest temperatures.)  $E_{\text{NMR}}$  and  $\tau_\infty$  are fitting parameters. It is convenient to define  $\tilde{\tau}_0 = (2\pi/3)(2I/E_{\text{NMR}})^{1/2}$ , where  $I$  is the moment of inertia of a methyl group. This simply assumes  $\tilde{\tau}_0^{-1}$  is an attempt (angular) frequency in a harmonic oscillator approximation.<sup>57</sup> The preexponential factor for hopping motion is much discussed in the literature and a variety of models results in expressions for  $\tilde{\tau}_0$  that are, to within a factor of 2 or 3, the same as the expression given by the harmonic model.<sup>13,16,57</sup> With this definition of  $\tilde{\tau}_0$ ,  $\tau_\infty/\tilde{\tau}_0$  becomes the fitting parameter and it should be within an order of magnitude or so of unity.

The simplest random hopping motion models for an ensemble of methyl rotors all characterized by the same environment and therefore by the same NMR activation energy,  $E_{\text{NMR}}$ , predicts that  $J(\omega, \tau)$  is given by the Debye (or Poisson or Bloembergen-Purcell-Pound) spectral density<sup>31,32,54</sup>  $J(\omega, \tau) = 2\tau/(1 + \omega^2\tau^2)$  which follows from using Poisson statistics to describe the rotational process.<sup>30,39-41</sup>

There are three adjustable parameters used in fitting the relaxation rate data:  $E_{\text{NMR}}$ ,  $C/\tilde{C}$ , and  $\tau_\infty/\tilde{\tau}_0$ . The parameter  $E_{\text{NMR}}$  should be in the range 8–16 kJ mol<sup>-1</sup> for the types of solids of which 4,4'-dimethoxybiphenyl is an example.<sup>20,49,50,58-63</sup> The parameter  $C/\tilde{C}$  should be approximately 1, or perhaps somewhat larger if the time dependence of methyl <sup>1</sup>H nuclei–nonmethyl <sup>1</sup>H nuclei vectors is significant. The parameter,  $\tau_\infty/\tilde{\tau}_0$ , should be within an order of magnitude of unity.

## IV. EXPERIMENTAL RESULTS

### A. Exponential NMR relaxation: the single exponential $R$

The relaxation is exponential to within experimental uncertainty at low temperatures and the recovery of the perturbed magnetization,  $M(t)$ , was fitted to  $M(t) = M(\infty)[1 - (1 - \cos\theta)\exp(-Rt)]$ .  $M(\infty)$  is the equilibrium magnetization and the adjustable parameter,  $\theta$ , accounts for imperfections in the perturbing inversion  $\pi$  pulse. That is, in the ideal case,  $(1 - \cos\theta) = 2$  if  $\theta = \pi$ . [ $M(0)$ , the initial magnetization after the perturbation, could be used as a fitting parameter instead of  $\theta$ .] We note that in these experiments, exponential relaxation involves a three-parameter fit:  $R$ ,  $\theta$  [or  $M(0)$ ], and  $M(\infty)$ . The rates,  $R$ , are shown to the right of the vertical lines in Figs. 1 and 2 and these regions are repeated in Fig. 3. The uncertainties in the values of  $R$  are very small and uncertainty bars are within the sizes of the symbols for  $R$  in Figs. 1–3 and as such are not visible.

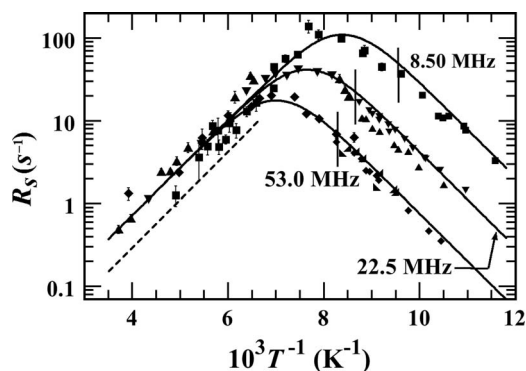


FIG. 2. The <sup>1</sup>H short-time (initial recovery) exponential relaxation rate,  $R_S$ , versus inverse temperature,  $T^{-1}$ , in polycrystalline 4,4'-dimethoxybiphenyl at NMR frequencies  $\omega_0/2\pi = 8.50$  (■), 22.5 (▲, ▼), and 53.0 MHz (◆, ▲). The different symbols for 22.5 and 53.0 MHz indicate different groupings of experiment days indicating (at lower temperatures) slightly different structures on different groups of days. At temperatures below (i.e., to the right of) the approximate positions of the vertical lines,  $R_S$  and a single-exponential relaxation fit characterized by  $R$  are indistinguishable ( $R_S = R$ ). Where error flags are not shown, the experimental uncertainties are within the sizes of the symbols. The solid lines correspond to a single fit as discussed in the text. The dashed line indicates the high-temperature  $R^*$  values in Fig. 1. The data to the right of the vertical lines are the same in Figs. 1 and 2 and are shown on an expanded scale in Fig. 3.

### B. Stretched-exponential NMR relaxation: $R^*$ and $\beta$

The relaxation is nonexponential at high temperatures and the entire recovery curve is well characterized by a four-parameter stretched exponential,  $M(t) = M(\infty)[1 - (1 - \cos\theta)\exp\{- (R^*t)^\beta\}]$ . The stretched-exponential function was introduced (as a fitting function in a physical science context) in 1854 by Kohlrausch.<sup>24</sup> It was reintroduced in 1970.<sup>64</sup> The parameter,  $R^*$ , is “the characteristic relaxation rate” and the parameter,  $0 < \beta < 1$ , is the “stretching factor.”  $R^*$  versus  $T^{-1}$  is shown in Fig. 1 and  $\beta$  versus  $T^{-1}$  is shown in Fig. 4. When  $\beta > 0.95$  (to the right of the vertical lines in Fig. 1), stretched-exponential relaxation is indistinguishable from exponential

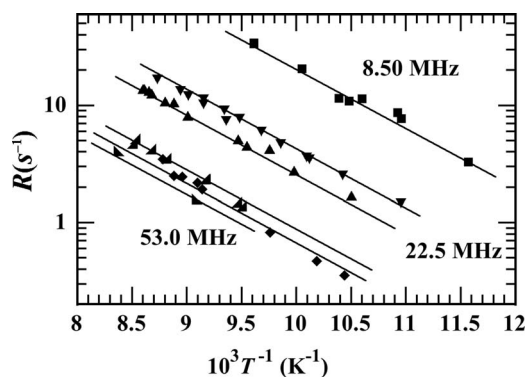


FIG. 3. The single-exponential <sup>1</sup>H relaxation rate,  $R$ , versus inverse temperature,  $T^{-1}$ , in polycrystalline 4,4'-dimethoxybiphenyl at NMR frequencies  $\omega_0/2\pi = 8.5$  (■), 22.5 (▲, ▼), and 53.0 MHz (◆, ▲) for temperatures below the vertical lines in Figs. 1 and 2. The relaxation is exponential in this regime. The different symbols for 22.5 and 53.0 MHz indicate different groupings of experiment days, indicating slightly different structures on different groups of days. The six lines are guides for the eye and all have the same slope of  $\ln R$  versus  $T^{-1}$ . All groups except the bottom line for 53.0 MHz involve two or more days of experiments. The experimental uncertainties are within the sizes of the symbols.

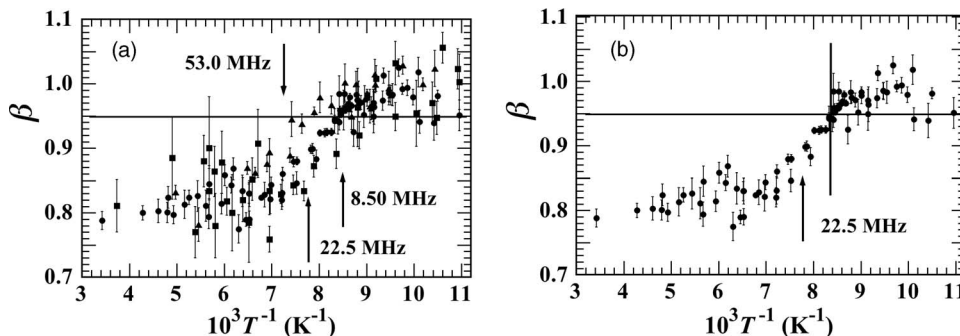


FIG. 4. The stretching parameter,  $\beta$ , versus inverse temperature,  $T^{-1}$ , for the  $^1\text{H}$  spin-lattice relaxation measurements in polycrystalline 4,4'-dimethoxybiphenyl.  $\beta = 1$  corresponds to exponential relaxation. To within experimental uncertainty, single-exponential relaxation is indistinguishable from stretched-exponential relaxation for  $\beta > 0.95$ , indicated by the horizontal lines. The vertical arrows indicate the values of the  $R^*$  maxima in Fig. 1. (a) Measurements at NMR frequencies  $\omega_0/2\pi = 8.50$  (■), 22.5 (●), and 53.0 MHz (▲). (b) Just the  $\omega_0/2\pi = 22.5$  MHz data.

relaxation in our experiments and, to within experimental uncertainty,  $R^* = R$ .

Figure 5 shows a magnetization  $M(t)$  decay for which  $\beta = 0.79 \pm 0.01$ . Figure 5(a) shows the relaxation curve with the inset showing shorter times. Figure 5(b) shows very short times. In all three plots in Figs. 5(a) and 5(b), a fit to both an exponential and a stretched exponential is shown. Figure 5(c) shows a difference plot; the difference between the observed  $M(t)$  and the fit to both a single ex-

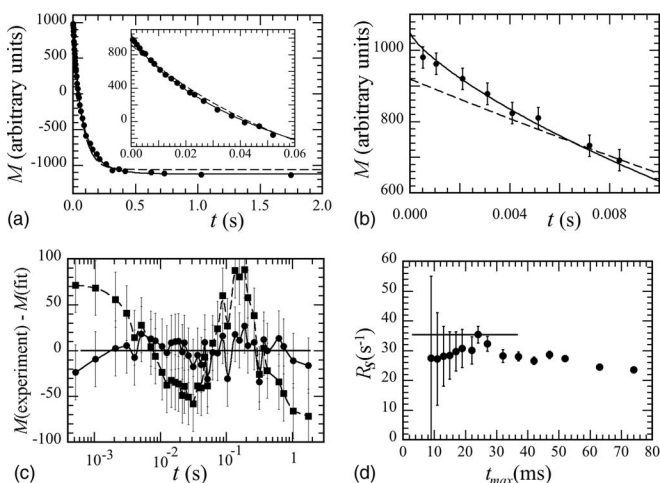


FIG. 5. An inversion recovery  $^1\text{H}$  nuclear spin-lattice relaxation experiment in polycrystalline 4,4'-dimethoxybiphenyl at an NMR frequency  $\omega_0/2\pi = 22.5$  MHz and at a temperature  $T = 155$  K ( $10^3 T^{-1} = 6.46$  K $^{-1}$ ). (a) and (b) The nuclear magnetization  $M$  versus time  $t$  between the perturbation  $\pi$  pulse and the measurement  $\pi/2$  pulse in an inversion recovery experiment. A stretched-exponential fit (solid line) gives  $R^* = 14.0 \pm 0.2$  s $^{-1}$  (see Fig. 1) and  $\beta = 0.79 \pm 0.01$  (see Fig. 4). A single exponential (dashed line) is a poor fit to the relaxation curve. The inset in (a) shows the first 60 ms. (b) The first 9 ms. The uncertainties for both the main plot and the inset in (a) are within the size of the symbols. The uncertainties can be seen in (b). (c) The difference between the observed and fitted  $M(t)$  values for the stretched-exponential (●) and single exponential (■) fits in (a) and (b). The logarithmic time scale is used solely to spread the data out. The lines joining the values are guides for the eye. The data in parts (a), (b), and (c) have the same uncertainties. (d) The single-exponential relaxation rate,  $R_S$ , that characterizes the short-time magnetization recovery versus the maximum time,  $t_{\text{max}}$ , used in the determination of  $R_S$ . The  $R_S$  value (used in Fig. 2) for this experiment is taken to be  $R_S = 35.4 \pm 2.8$  s $^{-1}$  as indicated by the datum going through the horizontal line.

ponential and to a stretched exponential. The sole purpose of the logarithmic time scale in Fig. 5(c) is so the data can be clearly seen at all time scales. [Fig. 5(d) is discussed below.] We suggest that a less careful study would not observe the departures from exponential relaxation. For completeness, we note that when the relaxation is nonexponential, a double exponential  $M(t) = M_1(\infty)[1 - (1 - \cos\theta)\exp(-R_1 t)] + M_2(\infty)[1 - (1 - \cos\theta)\exp(-R_2 t)]$ , provides a fit visually identical to the stretched exponential. However, whereas the stretched exponential is a four-parameter fit (and implies a continuous distribution of relaxation rates<sup>65,66</sup>), the double exponential is a five-parameter fit. In addition, the fit for the double exponential returns very large uncertainties for  $M_1(\infty)$  and  $M_2(\infty)$  (though their sum is determined quite accurately), which indicates that a five-parameter fit is unnecessary and models based on it may be unjustified.

One origin of the stretched exponential is that it is not an intrinsically fundamental function (i.e., as in the solution of a differential equation that models the dynamics) but rather an excellent approximation to either a hierarchy of an effectively infinite number of (exponential) relaxation rates or a distribution of independent (exponential) relaxation rates.<sup>65,66</sup> It has found use in interpreting neutron scattering experiments,<sup>67,68</sup> Kerr-effect spectroscopy in liquids,<sup>69</sup> studies of glass-forming liquids,<sup>70</sup> dielectric relaxation,<sup>71–75</sup> luminescence spectroscopy,<sup>76,77</sup> linear dichroism correlation spectroscopy,<sup>78</sup> lipid bilayer dynamics,<sup>79</sup> NMR spin-lattice relaxation in a random Heisenberg chain,<sup>80</sup> light scattering,<sup>74,75</sup> ion conductivity measurements,<sup>81</sup> NMR studies of ion conduction,<sup>82,83</sup> photobleaching relaxation,<sup>84</sup> and various forms of structural relaxation.<sup>85,86</sup>

It is not straightforward to relate the parameters  $R^*$  and  $\beta$  to the dynamics. If taken as a correlation function, the function  $\exp\{-(R^*t)^\beta\}$  cannot be Fourier transformed in closed form for arbitrary  $\beta$  and much effort has gone into relating it, or its numerically determined Fourier transform, to other functions such as the phenomenological Davidson-Cole function.<sup>75,86,87</sup> Also, much effort has gone into determining a distribution of exponential relaxation rates that gives the stretched exponential.<sup>88,89</sup> The best one can do is to relate  $R^*$  to a distribution function describing the fraction of relaxors with (an exponential) relaxation rate below  $R^*$  and the

fraction above  $R^*$ . ( $R^*$  should *not* be called the average relaxation rate.) But even then, these distribution functions depend on  $\beta$ . The meaning of  $\beta$  as a general parameter is even less clear than the meaning of  $R^*$  although certain specific values have been studied.  $\beta = 1$  corresponds to exponential relaxation. The cases of  $\beta = 2/3$ ,  $1/2$ , and  $1/3$  have been investigated very thoroughly and the distribution of exponential relaxation rates can be expressed in closed form using gamma functions and generalized hypergeometric functions.<sup>88,89</sup> For  $\beta < 1$ , the stretched-exponential function is unphysical at short times,<sup>65,70,71,76,77</sup> or, equivalently, at high frequencies<sup>69,71</sup> and this can be addressed by phenomenologically multiplying it by the appropriate function<sup>65,69,71</sup> or by shifting the time origin.<sup>76,77</sup> Our NMR relaxation experiments do not involve times short enough for this to be a problem. Finally, a very interesting topological approach to stretched-exponential relaxation that relates  $\beta$  to the dimensionality of the system has been presented.<sup>90</sup>

### C. The determination of the initial recovery rate, $R_S$ , for the nonexponential NMR relaxation

$R_S$  characterizes the initial magnetization decay following a perturbation. Fig. 2. shows  $R_S$  versus inverse temperature,  $T^{-1}$ . If the relaxation is nonexponential and the magnetization recovery is limited to smaller and smaller times after the perturbation, eventually the relaxation will be seen to be exponential to within experimental uncertainty.  $R_S$  is the rate to which the Bloch-Wangsness-Redfield model pertains. At temperatures below those indicated by the vertical lines in Figs. 1 and 2, the relaxation is exponential and  $R_S = R^* = R$ . Some of the uncertainties in  $R_S$  at higher temperatures are appreciable, especially at an NMR frequency of  $\omega_0/2\pi = 8.50$  MHz, as seen in Fig. 2.

$R_S$  was determined by fitting the relaxation to a single exponential and observing the “goodness of fit” and the fractional uncertainty in  $R_S$  as the maximum time,  $t$  (called  $t_{\max}$ ), between the perturbation  $\pi$  pulse and the observing  $\pi/2$  pulse used in the fit was decreased. Values of  $[t, M(t)]$  between the smallest  $t$  value [typically 500  $\mu$ s which is the case in Fig. 5(c)] and  $t_{\max}$  were used to determine  $R_S$ . This process is outlined in Fig. 5(d). At large values of  $t_{\max}$  the relaxation is nonexponential and as  $t_{\max}$  is decreased, the value of  $R_S$  gets larger and the relaxation becomes more exponential. In Fig. 5, for example, the complete data set has  $t_{\max} = 1.75$  s [Fig. 5(a)] and when  $t_{\max}$  is reduced to 76 ms [Fig. 5(d)], the relaxation appears to be well fitted by a single exponential with a value of  $R = 24$  s<sup>-1</sup>, with a very small uncertainty [within the size of the symbol in Fig. 5(d)]. As  $t_{\max}$  is decreased further,  $R_S$  becomes larger as does the uncertainty as outlined in Fig. 5(d). Eventually, the uncertainties become very large, in part because the number of data points used in the fit gets small and in part because the range in  $t$  gets so small that the relaxation curve is approaching a linear function. Although the equivalent of Fig. 5(d) looks slightly different for the very many runs performed at higher temperatures, in each case a reasonable value of  $R_S$  emerges. For the data in Fig. 5(d),  $t_{\max} = 24$  ms was chosen and this gives  $R_S = 35.4 \pm 2.8$  s<sup>-1</sup>. A less careful experiment taking  $t$  to 76 ms would conclude that the relax-

ation is exponential with  $R = 24$  s<sup>-1</sup> (and with a very small uncertainty), which would lead to an error of approximately 32%. Only if  $t$  were taken to much longer values would the practitioner realize that the relaxation was nonexponential.

### D. The results at lower temperature—different states?

At temperatures below 100–120 K (depending on NMR frequency), where the relaxation is strictly exponential, different sets of relaxation rates  $R$  versus temperature  $T$  were observed in different groups of days as can be seen in Figs. 1 and 2 and more clearly on the expanded plot in Fig. 3. Fig. 3 shows several parallel lines, all guides for the eye, for different sets of  $R$  versus  $T$  observed on different groups of days. All lines in Fig. 3 have the same slope of  $\ln R$  versus  $T^{-1}$ . The different lines for NMR frequencies  $\omega_0/2\pi = 22.5$  and 53.0 MHz suggest slightly different structures, either molecular, crystal, or both. As outlined in Sec. II, we checked carefully that the observed differences were not a result of systematic effects associated with certain probe plus sample plus thermocouple combinations.

### E. The fitted relaxation rate parameters

$R_S = R = (n/N) C [J(\omega_0, \tau) + 4J(2\omega_0, \tau)]$  can be used for the initial recovery of the nuclear magnetization at temperatures above 100–120 K (depending on NMR frequency) or the entire magnetization curve at temperatures below 100–120 K.  $J(\omega, \tau) = 2\tau / (1 + \omega^2\tau^2)$  with the mean time between hops  $\tau = \tau_\infty \exp(E_{\text{NMR}}/kT)$ . There are three fitting parameters:  $C$ ,  $E_{\text{NMR}}$ , and  $\tau_\infty$ . With  $\tilde{C} = (9/40)(\mu_0/4\pi)^2(\hbar\gamma^2/r^3)^2$  and  $\tilde{\tau}_\infty = (2\pi/3)(2I/E_{\text{NMR}})^{1/2}$ ,  $C/\tilde{C}$  and  $\tau_\infty/\tilde{\tau}_\infty$  replace  $C$  and  $\tau_\infty$  as fitting parameters. The Poisson spectral density,  $J(\omega, \tau) = 2\tau / (1 + \omega^2\tau^2)$ , requires that the magnitude of the slope of  $\ln R_S$  versus  $T^{-1}$  be the same at low and high temperatures. The fit shown for  $R_S$  in Fig. 2 gives  $E_{\text{NMR}} = 11.5 \pm 0.5$  kJ mol<sup>-1</sup>,  $C/\tilde{C} = 1.0 \pm 0.1$ , and  $\tau_\infty/\tilde{\tau}_\infty = 0.80 \pm 0.15$ . The fitted value of  $C/\tilde{C} = 1.0 \pm 0.1$  suggests that, to within experimental uncertainty, the model is appropriate and that only intramethyl <sup>1</sup>H spin–<sup>1</sup>H spin interactions need to be taken into account. In addition, the fitted value of  $\tau_\infty/\tilde{\tau}_\infty = 0.80 \pm 0.15$  is in good agreement with the simplest model where  $\tilde{\tau}_\infty^{-1}/2\pi$  is interpreted as a methyl group librational frequency at the bottom of the potential well.

This theoretical model for  $R_S$  versus  $T^{-1}$  in Fig. 2 does *not* apply to  $R^*$  versus  $T^{-1}$  in Fig. 1, but we use it to compare the two graphs. The high temperature fit in Fig. 1 is indicated by the dashed line in Fig. 2 and vice-versa. The low temperature data is the same in both figures.  $R^*$  is significantly smaller than  $R_S$  in the vicinity of the relaxation rate maximum and at higher temperatures. Although doing so has no justification, fitting the  $R^*$  versus  $T^{-1}$  curve with the same expression used for the  $R_S$  versus  $T^{-1}$  curve gives the same value for  $E_{\text{NMR}}$  but now  $C/\tilde{C} = 0.70 \pm 0.07$  and  $\tau_\infty/\tilde{\tau}_\infty = 0.55 \pm 0.15$ . These fitted parameters have no interpretation, but it is interesting to note that to within experimental uncertainty,  $R_S$  versus  $T^{-1}$  and  $R^*$  versus  $T^{-1}$  can be fitted with the same NMR activation energy,  $E_{\text{NMR}}$ . But a value of  $C/\tilde{C} = 0.70 \pm 0.07$  is not

physically possible. So long as accurate values for the intramethyl group H–H distances are used, a value of  $C/\tilde{C} < 1$  is not possible. This is explained in Sec. IV F.

### F. The sensitivity of the strength parameter $\tilde{C}$ on the H–H distance in a methyl group

The theoretical NMR strength parameter  $\tilde{C} = (9/40)(\mu_0/4\pi^2)^2(\hbar\gamma^2/r^3)^2$  is proportional to  $r^{-6}$ , where  $r$  is the distance between hydrogen atoms in the methyl groups (all of which are equivalent in crystalline 4,4'-dimethoxybiphenyl). So, in computing the strength parameter, care needs to be taken to determine  $r$  as accurately as possible. The values of  $r$  determined from electronic structure calculations in a suitable cluster of molecules based on the x-ray structure determination of the positions of the carbon and oxygen atoms,<sup>25</sup> are 175.4, 175.9, and 176.4 pm for an average of  $\langle r \rangle = \langle r^6 \rangle^{(1/6)} = 175.9$  pm. (None of the variations here are great enough for  $\langle r \rangle$  and  $\langle r^6 \rangle^{(1/6)}$  to be different to four significant figures.) This is to be compared with 178.9, 178.2, and 178.1 pm ( $\langle r \rangle = \langle r^6 \rangle^{(1/6)} = 178.4$  pm) as determined from electronic structure calculations in the isolated molecule<sup>25</sup> and with 160.0, 160.1, and 160.1 pm ( $\langle r \rangle = \langle r^6 \rangle^{(1/6)} = 160.1$ ) as determined by the software that places the hydrogen atoms in “ideal positions” in the single-crystal x-ray diffraction experiment.<sup>25</sup> Because of the weakness of the diffraction signal from hydrogen atoms (no core electron and a single valence electron), the positions and occupancies are difficult to measure accurately by x-ray crystallography. In addition, due to thermal vibrations, C–H bond lengths are apparently shortened in x-ray and neutron crystal structures. The shortening could be as large as 3 pm for C–H bond lengths in methyl groups in neutron diffraction measurements. C–H bond lengths obtained from x-ray diffraction are known to be shortened by more than 10 pm.<sup>91</sup> Indeed, if we used the x-ray values,  $r$  would be 10% too short and therefore the theoretical strength parameter  $\tilde{C}$  (proportional to  $r^{-6}$ ) would be 60% too large. One would then find that the experimentally determined strength parameter,  $C/\tilde{C}$ , is more than a factor of two, too small, and this would lead to an impossible conclusion. Even if the  $r$  values determined by electronic structure calculations in the isolated molecule were used, the small error in  $r$  would be 1.4% resulting in an 8.5% error in  $\tilde{C}$ . There may be additional methyl <sup>1</sup>H spin–nonmethyl <sup>1</sup>H spin interactions that could make the observed strength parameter  $C$  greater than  $\tilde{C}$ , the theoretically calculated parameter that assumes intramethyl interactions only but not the other way around. The computed value of  $\tilde{C}$  considers only the intramethyl spin-spin interactions and therefore has to be a minimum value, so long as the  $r$  values are accurate. As such, it is important to use the positions for the hydrogen atoms computed from electronic structure calculations in a cluster made from the structure determined by x-ray diffraction or neutron scattering.<sup>25</sup>

### V. CONCLUSIONS AND SUMMARY

Fitting the <sup>1</sup>H NMR nuclear spin-lattice relaxation data for 4,4'-dimethoxybiphenyl provides an activation energy for methyl group rotation of  $11.5 \pm 0.5$  kJ mol<sup>-1</sup>. This value is

in reasonable agreement with the value of 10.3 kJ mol<sup>-1</sup> determined from the electronic structure calculations in an appropriate cluster of molecules.<sup>25</sup> The NMR parameter that characterizes the strength of the dipole-dipole interactions whose modulation is responsible for the relaxation agrees very well with data obtained from the experiment but only if one uses the “correct” value for the H–H distances in a methyl group; namely those obtained from electronic structure calculations in a cluster of molecules based on the x-ray determination of the atomic positions of all atoms except hydrogen atoms.<sup>25</sup>

On different groups of days, we observed statistically different  $\ln R$  versus  $T^{-1}$  regions (for relaxation rate  $R$  and temperature  $T$ ) at lower temperatures where the relaxation was exponential and could, therefore, be characterized very accurately. This presumably results from very slight differences in the molecular conformation, the crystal structure, or both.<sup>26</sup> Very small differences in H–H separations,  $r$ , have a huge effect since the interactions that enter the expressions for the observed relaxation rates are proportional to  $r^{-6}$ . There are cases where different polymorphs have very different observed  $R$  versus  $T^{-1}$  curves<sup>29,30</sup> and there are cases, such as that observed here and elsewhere,<sup>15,92</sup> where small changes in the observed  $R$  versus  $T^{-1}$  curves have yet to be correlated with different structures determined from x-ray diffraction. <sup>1</sup>H NMR relaxation in the solid state is probably much more sensitive to small structural changes than either neutron scattering or x-ray diffraction. However, the technique cannot appropriately characterize the state.

We showed how very well a stretched-exponential function fits nonexponential relaxation data while introducing only one additional adjustable parameter (when compared with exponential relaxation). A brief literature review of the use of the stretched-exponential function was given in Sec. IV B. However, this fitting function is nothing more than a convenient phenomenological representation of the data and the resulting parameters that characterize the relaxation are not amenable to interpretation in any meaningful way at this time aside from saying that they characterize a distribution of relaxation rates in a manner that cannot be related to a particular model. Indeed, we showed that if the stretched-exponential characteristic relaxation rates were used instead of the significantly greater values of the relaxation rates obtained from an initial recovery of the perturbed nuclear magnetization, the fitted NMR strength parameter changed by 30% and was lower than its smallest possible theoretical value.

Some studies interpret nonexponential relaxation in terms of the sum of two exponentials, which involves one more adjustable parameter than a stretched-exponential function (and two more than exponential relaxation). If this interpretation of the data is driving a subsequent model (i.e., two kinds of relaxors), then it should be determined that a stretched exponential (implying a continuous distribution of relaxors) does not fit the data.

We noted that in regions where the nuclear spin-lattice relaxation is nonexponential, if an automated program were used to provide a single-exponential relaxation rate, the program might very well return an incorrect value. Unless the



experimenter looked closely at the data, the nonexponentiality would not be seen and the rate determined could be significantly lower (by more than 30% in the case presented here) than a value obtained from the appropriate initial slope. The message here is to use a large range in time and carefully visually inspect the fit, do not simply trust the parameters and the uncertainties delivered by a nonlinear fitting algorithm.

## ACKNOWLEDGMENTS

We thank Sally Mallory in the Chemistry Department at the University of Pennsylvania and Frank Mallory in the Chemistry Department at Bryn Mawr College for recrystallizing the samples used and for very helpful discussions. We also thank Xianlong Wang of the University of Electronic Science and Technology of China in Chengdu for very helpful discussions.

- <sup>1</sup>J. Haupt, *Zeitschrift für Naturforschung A* **26a**, 1578 (1971).
- <sup>2</sup>G. Diezemann, *Appl. Magn. Reson.* **17**, 345 (1999).
- <sup>3</sup>M. J. Barlow, S. Clough, A. J. Horsewill, and M. A. Mohammed, *Solid State Nucl. Magn. Reson.* **1**, 197 (1992).
- <sup>4</sup>S. Clough, *Physica B* **136**, 145 (1986).
- <sup>5</sup>S. Clough and P. J. McDonald, *J. Phys. C* **15**, L1039 (1982).
- <sup>6</sup>S. Clough, A. Heidemann, A. J. Horsewill, J. D. Lewis, and M. N. J. Paley, *J. Phys. C* **15**, 2495 (1982).
- <sup>7</sup>S. Clough, A. Heidemann, A. J. Horsewill, J. D. Lewis, and M. N. J. Paley, *J. Phys. C* **14**, L525 (1981).
- <sup>8</sup>P. A. Beckmann and S. Clough, *J. Phys. C* **11**, 4055 (1978).
- <sup>9</sup>P. A. Beckmann, S. Clough, J. W. Hennel, and J. R. Hill, *J. Phys. C* **10**, 729 (1977).
- <sup>10</sup>S. Clough, *Solid State Nucl. Magn. Reson.* **9**, 49 (1997).
- <sup>11</sup>S. Clough, P. J. McDonald, and F. O. Zelaya, *J. Phys. C* **17**, 4413 (1984).
- <sup>12</sup>D. Cavagnat, S. Clough, and F. O. Zelaya, *J. Phys. C* **18**, 6457 (1985).
- <sup>13</sup>S. Clough and A. Heidemann, *J. Phys. C* **13**, 3585 (1980).
- <sup>14</sup>E. O. Stejskal and H. S. Gutowsky, *J. Chem. Phys.* **28**, 388 (1958).
- <sup>15</sup>P. A. Beckmann, W. G. Dougherty, Jr., and W. S. Kassel, *Solid State Nucl. Magn. Reson.* **36**, 86 (2009).
- <sup>16</sup>P. A. Beckmann, J. Rosenberg, K. Nordstrom, C. W. Mallory, and F. B. Mallory, *J. Phys. Chem. A* **110**, 3947 (2006).
- <sup>17</sup>P. A. Beckmann, C. Dybowski, E. J. Gaffney, C. W. Mallory, and F. B. Mallory, *J. Phys. Chem. A* **105**, 7350 (2001).
- <sup>18</sup>C. Palmer, A. M. Albano, and P. A. Beckmann, *Physica B* **190**, 267 (1993).
- <sup>19</sup>P. A. Beckmann, L. Happersett, A. V. Herzog, and W. M. Tong, *J. Chem. Phys.* **95**, 828 (1991).
- <sup>20</sup>K. G. Conn, P. A. Beckmann, C. W. Mallory, and F. B. Mallory, *J. Chem. Phys.* **87**, 20 (1987).
- <sup>21</sup>P. Gutsche, H. Schmitt, U. Haebleren, T. Ratajczyk, and S. Szymanski, *ChemPhysChem* **7**, 886 (2006).
- <sup>22</sup>L. K. Runnells, *Phys. Rev.* **134**, 28 (1964).
- <sup>23</sup>R. L. Hilt and P. S. Hubbard, *Phys. Rev.* **134**, 392 (1964).
- <sup>24</sup>R. Kohlrausch, *Ann. Phys. Chem. (Poggendorff)* **91**, 179 (1854).
- <sup>25</sup>X. Wang, L. Rotkina, H. Su, and P. A. Beckmann, "Single-crystal X-ray diffraction, isolated molecule and cluster electronic structure calculations, and scanning electron microscopy in an organic molecular solid: Models for intramolecular motion in 4,4'-dimethoxybiphenyl," *ChemPhysChem* (submitted).
- <sup>26</sup>S. Price, *Phys. Chem. Chem. Phys.* **10**, 1996 (2008).
- <sup>27</sup>A. Nangia, *Acc. Chem. Res.* **41**, 595 (2008).
- <sup>28</sup>J. Bernstein, *Polymorphism in Molecular Crystals* (Oxford University Press, Oxford, 2007).
- <sup>29</sup>P. A. Beckmann, K. S. Burbank, K. M. Clemo, E. N. Slonaker, K. Averill, C. Dybowski, J. S. Figueroa, A. Glatfelder, S. Koch, L. M. Liable-Sands, and A. L. Rheingold, *J. Chem. Phys.* **113**, 1958 (2000).
- <sup>30</sup>A. L. Rheingold, J. S. Figueroa, C. Dybowski, and P. A. Beckmann, *Chem. Comm.* **2000**, 651 (2000).
- <sup>31</sup>A. Abragam, *The Principles of Nuclear Magnetism* (Oxford University Press, Oxford, 1961).
- <sup>32</sup>N. Bloembergen, E. M. Purcell, and R. V. Pound, *Phys. Rev.* **73**, 679 (1948).
- <sup>33</sup>I. Solomon, *Phys. Rev.* **99**, 559 (1955).
- <sup>34</sup>A. G. Redfield, *IBM J. Res. Dev.* **1**, 19 (1957); reprinted with minor revisions in *Adv. Magn. Reson.* **1**, 1 (1965).
- <sup>35</sup>K. Tomita, *Prog. Theor. Phys.* **19**, 541 (1958).
- <sup>36</sup>F. Bloch, *Phys. Rev.* **102**, 104 (1956); **105**, 1206 (1957).
- <sup>37</sup>R. K. Wangsness and F. Bloch, *Phys. Rev.* **89**, 728 (1953).
- <sup>38</sup>D. E. Woessner, *J. Chem. Phys.* **36**, 1 (1955).
- <sup>39</sup>C. P. Slichter, *Principles of Magnetic Resonance*, 3rd ed. (Springer-Verlag, Berlin, 1990).
- <sup>40</sup>R. R. Ernst, G. Bodenhausen, and A. Wokaum, *Principles of Nuclear Magnetic Resonance in One and Two Dimensions* (Oxford University Press, Oxford, 1987).
- <sup>41</sup>R. Kimmich, *NMR Tomography, Diffusometry, Relaxometry* (Springer-Verlag, Berlin, 1997).
- <sup>42</sup>M. Goldman, *J. Magn. Reson.* **149**, 160 (2001).
- <sup>43</sup>M. Mehring and H. Raber, *J. Chem. Phys.* **59**, 1116 (1973).
- <sup>44</sup>J. D. Cutnell and W. Venable, *J. Chem. Phys.* **60**, 3795 (1974).
- <sup>45</sup>M. F. Baud and P. S. Hubbard, *Phys. Rev.* **170**, 384 (1968).
- <sup>46</sup>L. J. Burnett and B. H. Muller, *Chem. Phys. Lett.* **18**, 553 (1973).
- <sup>47</sup>P. S. Hubbard, *J. Chem. Phys.* **51**, 1647 (1969).
- <sup>48</sup>A. Kumar and C. S. Johnson, Jr., *J. Chem. Phys.* **60**, 137 (1974).
- <sup>49</sup>X. Wang, A. L. Rheingold, A. G. DiPasquale, F. B. Mallory, C. W. Mallory, and P. A. Beckmann, *J. Chem. Phys.* **128**, 124502 (2008).
- <sup>50</sup>P. A. Beckmann, C. A. Buser, C. W. Mallory, F. B. Mallory, and J. Mosher, *Solid State Nucl. Magn. Reson.* **12**, 251 (1998).
- <sup>51</sup>N. Pislewski, J. Tritt-Goc, M. Bielejewski, A. Rachocki, T. Ratajczyk, and S. Szymanski, *Solid State Nucl. Magn. Reson.* **35**, 194 (2009).
- <sup>52</sup>C. Sun and A. J. Horsewill, *Solid State Nucl. Magn. Reson.* **35**, 139 (2009).
- <sup>53</sup>T. Fukunaga, N. Kumagai, and H. Ishida, *Zeitschrift für Naturforschung A* **58a**, 631 (2003).
- <sup>54</sup>P. A. Beckmann, *Phys. Rep.* **171**, 85 (1988).
- <sup>55</sup>D. I. Hoult, *Concepts Magn. Reson. Part A* **34**, 193 (2009).
- <sup>56</sup>F. Engelke, *Concepts Magn. Reson. Part A* **36**, 266 (2010).
- <sup>57</sup>N. L. Owen, in *Internal Rotation in Molecules*, edited by W. J. Orville-Thomas (Wiley, New York, 1974), p. 157.
- <sup>58</sup>P. A. Beckmann, K. S. Burbank, M. M. W. Lau, J. N. Ree, and T. L. Weber, *Chem. Phys.* **290**, 241 (2003).
- <sup>59</sup>J. A. Weiss and P. A. Beckmann, *Solid State Nucl. Magn. Reson.* **16**, 239 (2000).
- <sup>60</sup>M. T. Myaing, L. Sekaric, and P. A. Beckmann, *Zeitschrift für Naturforschung A* **52a**, 757 (1997).
- <sup>61</sup>A. L. Plofker and P. A. Beckmann, *J. Phys. Chem.* **99**, 391 (1995).
- <sup>62</sup>H. A. Al-Hallaq and P. A. Beckmann, *J. Chem. Soc. Faraday Trans.* **89**, 3801 (1993).
- <sup>63</sup>F. B. Mallory, C. W. Mallory, K. G. Conn, and P. A. Beckmann, *J. Chem. Phys. Solids* **51**, 129 (1990).
- <sup>64</sup>G. Williams and D. C. Watts, *Trans. Far. Soc.* **66**, 80 (1970).
- <sup>65</sup>R. M. Pickup, R. Cywinski, C. Pappas, B. Farago, and P. Fouquet, *Phys. Rev. Lett.* **102**, 097202 (2009). Reference 1 in this paper is incorrect. It should be Ref. 24 in this work.
- <sup>66</sup>R. G. Palmer, D. L. Stein, E. Abrahams, and P. W. Anderson, *Phys. Rev. Lett.* **53**, 958 (1984). (Ref. 1 in this paper is incorrect. It should be Ref. 24 in this work.)
- <sup>67</sup>M. Krutyeva, J. Martin, A. Arbe, J. Colmenero, C. Mijangos, G. J. Schneider, T. Unruh, Y. Su, and D. Richter, *J. Chem. Phys.* **131**, 174901 (2009).
- <sup>68</sup>J. C. Phillips, *Rep. Prog. Phys.* **59**, 1133 (1996). (The Kohlrausch reference in this paper is incorrect. It should be Reference 24 in this work.)
- <sup>69</sup>D. A. Turton and K. Wynne, *J. Chem. Phys.* **131**, 201101 (2009).
- <sup>70</sup>C. M. Roland and K. L. Ngai, *J. Chem. Phys.* **103**, 1152 (1995).
- <sup>71</sup>J. G. Powles, D. M. Heyes, G. Rickayzen, and W. A. B. Evans, *J. Chem. Phys.* **131**, 214509 (2009).
- <sup>72</sup>V. Halpern, *J. Chem. Phys.* **124**, 214508 (2006).
- <sup>73</sup>K. L. Ngai, *Phys. Rev. B* **71**, 214201 (2005).
- <sup>74</sup>J. L. Skinner, *J. Chem. Phys.* **79**, 1955 (1983).
- <sup>75</sup>C. P. Lindsey and G. D. Patterson, *J. Chem. Phys.* **73**, 3348 (1980).
- <sup>76</sup>M. N. Berberan-Santos, *Chem. Phys. Lett.* **460**, 146 (2008).
- <sup>77</sup>M. N. Berberan-Santos, E. N. Bodunov, and B. Valeur, *Chem. Phys.* **315**, 171 (2005).
- <sup>78</sup>S. Adhikari, M. Selmke, and F. Cichos, *Phys. Chem. Chem. Phys.* **13**, 1849 (2011).
- <sup>79</sup>E. G. Brandt and O. Edholm, *J. Chem. Phys.* **133**, 115101 (2010).
- <sup>80</sup>T. Shiroka, F. Casola, V. Glazkov, A. Zheludev, K. Pra, H.-R. Ott, and J. Mesot, *Phys. Rev. Lett.* **106**, 137202 (2011).

- <sup>81</sup>D. L. Sidebottom, P. F. Green, and R. K. Brow, *J. Non-Cryst. Solids* **183**, 151 (1995).
- <sup>82</sup>M. Vogel, C. Brinkmann, H. Eckert, and A. Heuer, *Phys. Rev. B* **69**, 094302 (2004).
- <sup>83</sup>K. L. Ngai, *J. Non-Cryst. Solids* **162**, 268 (1993).
- <sup>84</sup>M. T. Cicerone and M. D. Ediger, *J. Phys. Chem.* **103**, 5684 (1995).
- <sup>85</sup>M. D. Ediger, C. A. Angell, and S. R. Nagel, *J. Phys. Chem.* **100**, 13200 (1996).
- <sup>86</sup>R. Kahlau, D. Kruk, Th. Blochowicz, V. N. Novikov, and E. A. Rossler, *J. Phys. C: Conden. Mat.* **22**, 365101 (2010).
- <sup>87</sup>T. C. Dotson, J. Budzien, J. D. McCoy, and D. B. Adolf, *J. Chem. Phys.* **130**, 024903 (2009). (Ref. 1 in this paper is incorrect. It should be Ref. 24 in this work.)
- <sup>88</sup>E. Helfand, *J. Chem. Phys.* **78**, 1931 (1983).
- <sup>89</sup>D. C. Johnston, *Phys. Rev. B* **74**, 184430 (2006).
- <sup>90</sup>J. R. Macdonald and J. C. Philips, *J. Chem. Phys.* **122**, 074510 (2005).
- <sup>91</sup>T. Steiner and W. Saenger, *Acta Crystallogr. A* **49**, 379 (1993).
- <sup>92</sup>P. A. Beckmann, C. Paty, E. Allocco, M. Herd, K. Kuranz, and A. L. Rheingold, *J. Chem. Phys.* **120**, 5309 (2004).